PEDOSTRATIGRAPHY, PEDOLOGICAL AND GEOCHEMISTRY OF KASHMIR LOESS: IMPLICATIONS FOR CHEMICAL WEATHERING HISTORY AND PALEOCLIMATIC RECONSTRUCTION

Rakesh Chandra
Ishtiaq Ahmad
Department of Earth Sciences, University of Kashmir, Srinagar, Jammu and Kashmir, India

Abstract:

Integrated pedological and geochemical study of the Quaternary Loess-Paleosols sediments of the Kashmir Valley was carried out in order to reconstruct their chemical weathering, paleoclimatological conditions and source. Pedological and micromorphic features of these paleosols indicate that these are weak to moderately developed. It also indicates that both loess deposition and pedogenic processes were taking place simultaneously during either phase of the loess/soil formation. These sediments are generally enriched with Fe_2O_3, MgO, MnO, TiO_2, Y, Ni, Cu, Zn, Th, Sc, V and Co while contents of SiO_2, K_2O, Na_2O, P_2O_5, Sr, Nb and Hf are lower than the UCC. Al_2O_3 is slightly higher than the UCC. However, CaO and U show large variations. Rb is generally similar to UCC whereas Ba is slightly lower than the UCC. Chondrite normalized REE patterns are characterized by moderate enrichment of LREEs, relatively flat HREE pattern (Gd_{CN}/Yb_{CN} = 1.93 to 2.30) and lack of prominent negative Eu anomaly (Eu/Eu* = 0.73 to 1.01, average = 0.81). The weathering indices suggest that these sediments are experiencing weak to moderate degree of weathering and not subjected to potash metasomatism. On the basis of these proxies it is inferred that the climate of Kashmir Valley for the recent past fluctuated between cold arid to warm semi-arid.

Key Words: Loess, Paleosols, weathering, Karewas, Kashmir

Introduction

Pleistocene loess deposits in the Kashmir Valley of the North Western Himalaya are the thickest and most extensive in Indian subcontinent. These loess deposits represent an important archive of terrestrial paleoenvironmental changes. Stratigraphically, the loess-paleosol sequence of the Kashmir Valley fall into two broad types: a thick sequence and a thin sequence. A thick sequence is about 21m thick and lie toward the southwest of the Kashmir Valley along the Pir-Panjal flank. This sequence consists of ten paleosols and three loess horizons (Ahmad, 2012). The thin sequence lies toward the northeastern part of the Kashmir Valley and contains four paleosols. This sequence is equivalent to the top part of the thicker sequence (Ahmad, 2012). Singhvi et al. (1987) proposed that the Kashmir loess sequence extended back to the 350ka B.P. However, Gupta et al. (1991) proposed much shorter framework and concluded that the base of the loess sequence is approximately 200ka B.P. In this paper we present the pedostratigraphy as well as pedological and geochemical characterization of the Kashmir Loess-Paleosol sequence. An attempt has also been made for paleoclimatic reconstruction.

Geological setting

Kashmir valley has the morphological characteristics of an intermountain basin and is located on a nearly horizontal Nappe sheet (Wadia, 1976). The valley is flanked by the Himalayas to the northeast and Pir-Panjal Range (Panjal Thrust) in the southwest. These mountainous ranges comprise metamorphosed Paleozoic and Mesozoic marine sediments and effusive rocks (Farooqi and Desai, 1974). The valley preserves the record of past 4 M.Y in which the sedimentation is controlled by the tectonic events. The valley possesses almost complete stratigraphic record of rocks of all ages ranging from Archean to Recent (Fig.1).

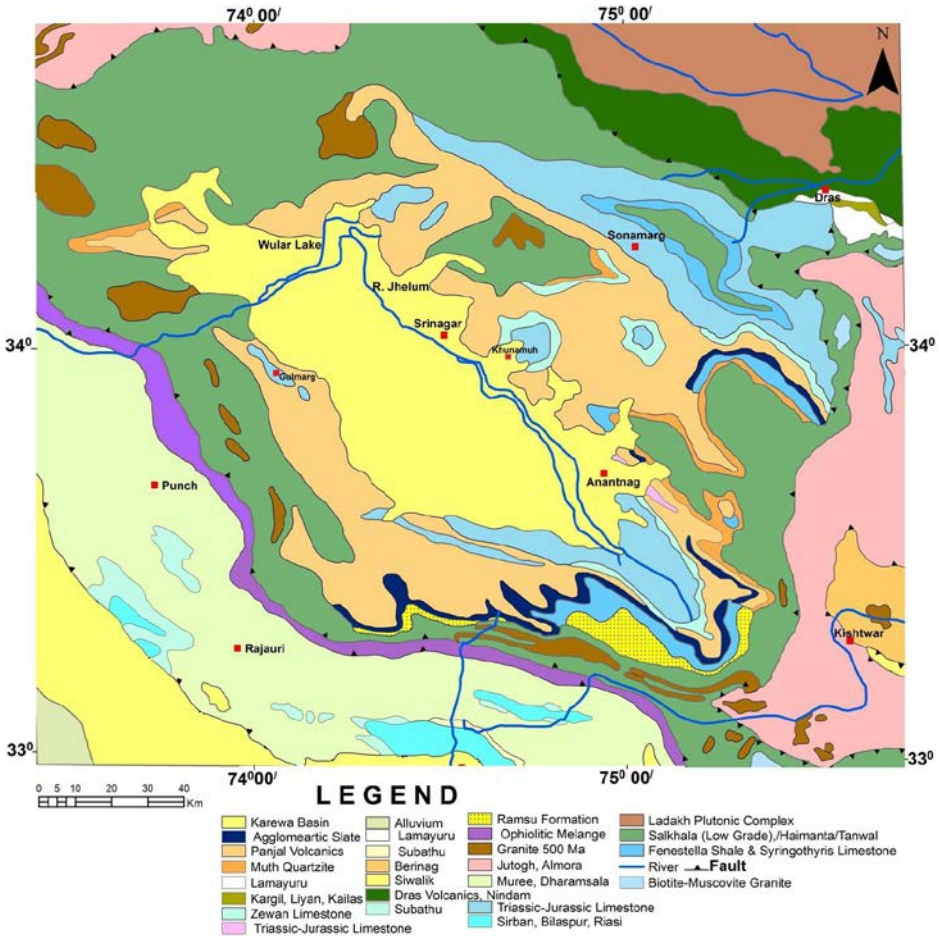

Fig.1. Geological map of Kashmir Himalaya (modified after Thakur and Rawat, 1992).

The Panjal Volcanic series and the Triassic limestone form the main geological formations and are underlain by the Archean metasedimentaries of Salkhala Formation (Fig.1). The Panjal Volcanic series of Permo-Carboniferous age is divisible in to two well marked horizons, the lower agglomeratic slate and the upper Panjal lava flows (Bhatt and Zainuddin, 1979). These oldest rocks are found around the northwestern extremity of the Kashmir valley and portions of the Pir-Panjal range. Exposures of Triassic rocks comprise alternate thick dark grey limestone and shally-arenaceous impure limestone. The other rocks of lesser distribution include Dogra Slates, Cambro-Silurian, Zewan Formation and Muth-Quartzites. The Precambrian to Mesozoic basement rocks in turn are overlain by Plio-Pleistocene sediments constituting the Karewa Group, which in turn capped by the loess sediments of Dilpur Formation.

Lithostratigraphy of Kashmir Loess-Paleosols

Three representative loess-paleosol containing sections have been selected for detailed study (Fig.2). On the basis of detailed field observations, four loess horizons with seven embedded paleosol profiles have been identified at Dilpur Village section. Karapur Village section contains ten paleosol profiles and three loess horizons. However, at Burzahom Village section four paleosol profiles have been found. Key macromorphological features of these sediments are illustrated in Fig.3. The paleosol profiles show low organic matter contents and weak to moderately developed illuvial clay pedofeatures, which suggests subtle climatic changes that affect relative rates of material supply and weathering rates. This further suggests that these paleosol profiles are formed when both loess deposition and pedogenic processes were taking place simultaneously during both stadial to interstadial phases, representing cold arid to warm semi-arid climate. Therefore, it is inferred that these paleosol profiles do not each represent a complete interglacial period (Gardner, 1989). The paleosol profiles DS3, KS4 and BS4 are relatively well developed and record maximum thickness, which represent warm semi-arid climate. The parent loess horizons are mostly absent at the base of these paleosol profiles (Fig.3). This indicates relative stable land surface conditions when the

pedogenic processes become more dominant and the parent loessic material transformed into illuvial ('B_t') horizon (Yakimenko et al. 2004). The lithological characteristics such as organic activities, illuvial pedofeatures and granularity of soil are relatively weakly developed at Dilpur village section as compared to Karapur and Burzahom village sections. However, the different types of calcretes such as $CaCO_3$ coating, infilling, platy concretions and nodules are relatively well developed at Dilpur Village section than Karapur Village section. Lithological characters reveal that the Dilpur Village section experienced relatively arid climatic conditions as compared to the Karapur and Burzahom Village sections. The Dilpur Village section is lower in altitude than Karapur and Burzahom

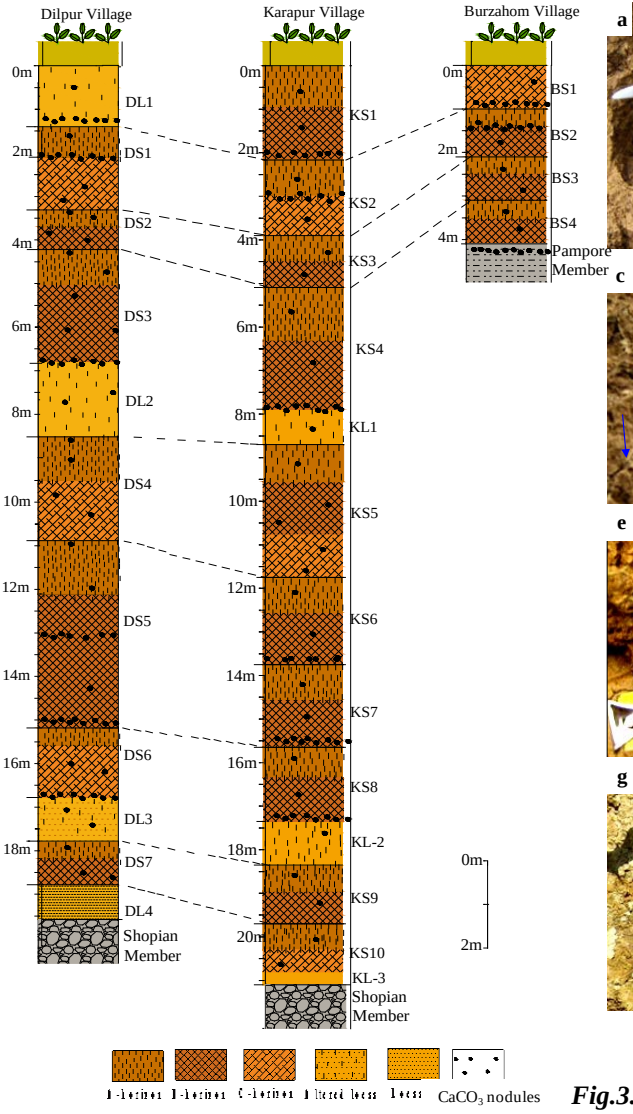

Fig.2. *Lithostratigraphic correlation of Kashmir Loess-Paleosol sediments at Dilpur, Karapur and Burzahom Village sections.*

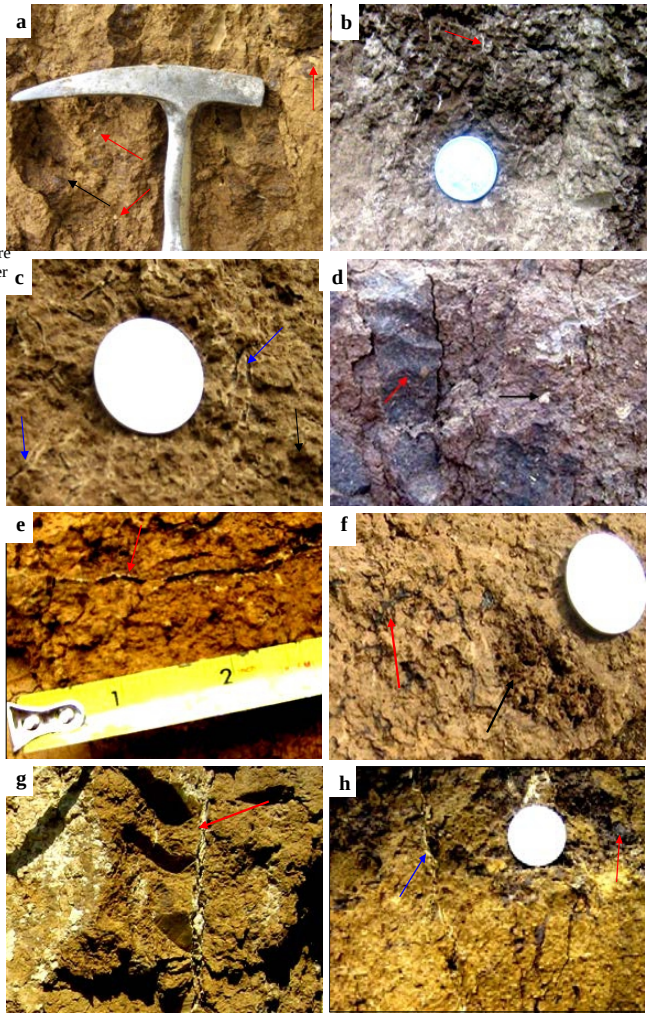

Fig.3. *Photograph showing (a) clay coating (black arrows) and calcareous nodules (red arrows) in paleosol profile DS5, (b) granular structures and root traces coated with $CaCO_3$ in paleosol profile DS7, (c) root traces coated with $CaCO_3$ in paleosol profile DS3, (d) clay coating (red arrow) and nodules of $CaCO_3$ (black arrow) in paleosol profile KS9, (e) root traces coated with $CaCO_3$ (arrow) in paleosol profile KS4, (f) burrows (red arrow) and root traces (black arrows) in paleosol profile KS7, (g) platy concretions in BS2 paleosol profile, (h) clay coating (red arrows) and platy concretion of $CaCO_3$ (blue arrow) in BS3 paleosol profile.*

Village sections and hence has high potential for evapo-transpiration. Hence, it experiences relatively dry climatic conditions than the Karapur and Burzahom Village sections. Therefore, the soil-water balance of these locations differs which affects the rate of pedogenesis (Bronger et al. 1987). This suggests that the local geographical conditions also played vital role in the pedogenic modification of these sediments (Bronger et al. 1987). Overall these loess-paleosol sediments show similar type of lithological characteristics although there is difference in degree of maturity of soil at different sections.

Micromorphology

The micromorphological study of three loess-paleosol containing sections of Kashmir Valley has been carried out to determine the pedogenic processes and climatic conditions prevailing during their development. Key micromorphological features of these loess and paleosols sediments are illustrated in Fig.4. The description refers to the most representative and typical micromorphological features of the about 150 thin sections. Presented here in detail are only the most typical pedofeatures with clear environmental implications. Among a large variety of microstructures, massive or apedal microstructures, channel microstructures, peds microstructures, spongy structure, textural pedofeatures, calcitic pedofeatures, basic mineral components and organic matter are the most common in the studied loess-paleosols sediments.

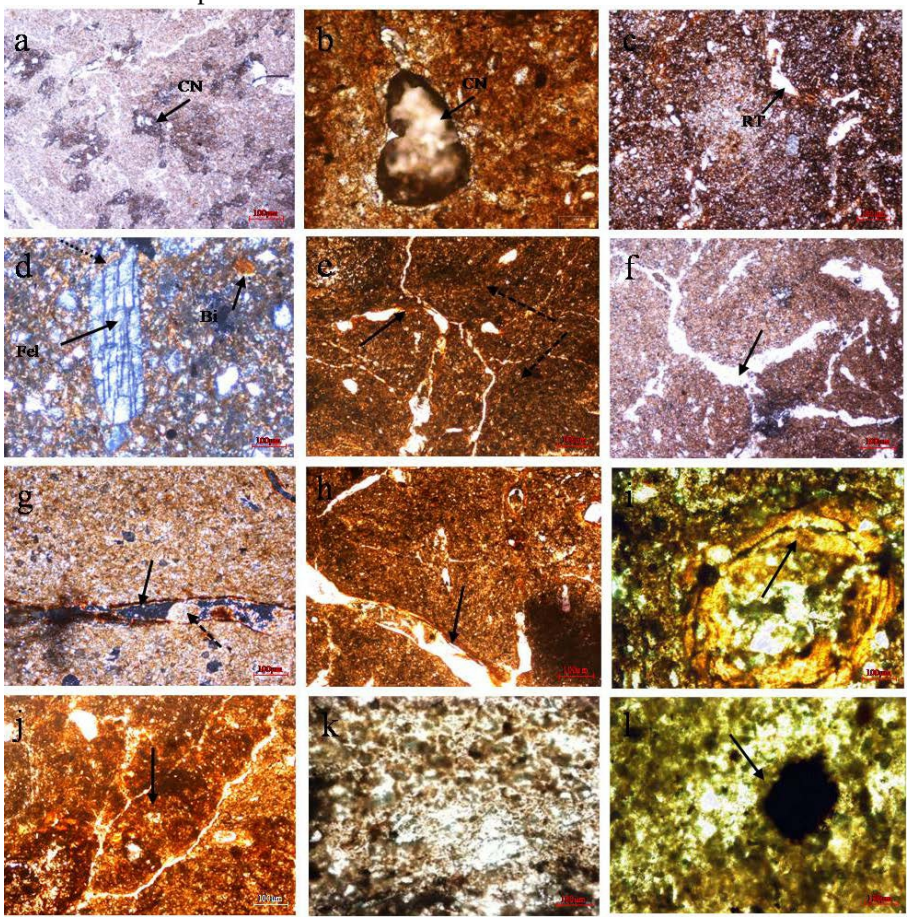

Fig.4. *Photomicrographs from Kashmir Loess-Paleosols at Dilpur, Karapur and Burzahom Village sections illustrating some key micromorphological features of the Kashmir Loess-Paleosols sediments. (a-b) massive structures with $CaCO_3$ nodules (CN) in D-L1 and K-L1 loess horizons respectively, (c) massive structures with disseminated organic matter and fine root traces (RT) in K-S2 horizon, (d) massive structures with thin clay coating around the skeleton grains (dotted arrow), feldspar (Fel) and partially altered biotite (Bi) in paleosol profile K-S10, (e) peds (dotted arrows) and limpid yellow brown clay coating along the channels (solid arrow) in paleosol profile D-S5, (f) fluid conducting channels coated with $CaCO_3$ in paleosol profile B-S1, (g) ferruginized plant remains (solid arrow) and $CaCO_3$ infillings (dotted arrow) in paleosol profile K-S5, (h) channels showing thick ferruginous clay coatings in paleosol profile D-S3, (i) rounded channels with alternate layers of thick limpid yellow clays in paleosol profile D-S3, (j) platy pedal microstructures in paleosol profile K-S5, (k) spongy microstructures in paleosol profile D-S2, and (l) spongy microstructures with Fe/Mn oxides in D-L3 loess horizon.*

Massive microstructures are generally observed in loess (Fig.4a,b) and weakly altered 'B_w' horizons of the sequences (Fig.4c,d), showing homogeneity and small porosity in the groundmass. Thin clay coating is also observed around the skeleton grains in 'B_w' horizons (Fig.4d), with finely disseminated organic matter assimilated with the groundmass (Fig.4c). The paleosols possessing these structures imply their subjection to only weak soil forming processes. However, channels mainly result from root growth (Zarate et al. 2000) and by the fluid migration within the profile (Fig.4e,f). These channels sometimes contain ferruginized plants remains with coatings, hypocoatings and infilling of secondary $CaCO_3$ (Fig.4g). This type of microstructure is generally found in weakly developed paleosol profiles (Li et al. 1992). In contrast, channels in the moderately developed paleosols profile are relatively large and more abundant (Fig.4h,i). All the paleosols show weak to moderate pedality along with large channel and platy peds microstructures (Fig.4e,j). These peds are formed by shrink-swell activities due to fluctuations in water saturation because of seasonal wetting and drying conditions (Kemp and Zarate, 2000). Spongy microstructure mainly results from strong biological activity. This is observed in the surface horizons of paleosol profiles DS2 and KS3 and loess horizon DL3 (Fig.4k,l). It is typically associated with surface (A) horizons of soils, so the presence of spongy microstructures in the lowermost 'C' horizons (Fig.4l) of the profile supports the accretionary nature whereby the loess was modified by bioturbation (and probably leaching) processes as it accumulated (Kemp et al. 2003). Rates of loess deposition eventually diminished to such an extent that a stable land surface was established and pedogenic processes became more dominant (Kemp et al. 2003). The soils with spongy microstructures can be regarded as weakly developed steppe soils in semi-arid environment (Zhengtang et al. 1996). Thick microlaminated clay coatings along large channel voids and thin clay coatings along planar voids or channel walls are common (Fig.4e). The secondary $CaCO_3$ nodules show clear boundaries to the groundmass (Fig.4b). The depth distribution of these features provides the basis for the modification of the horizon nomenclature and a reconstruction of the pedosedimentary events. Quartz is the dominant mineral in both paleosols and the parent loess material followed by feldspar (Fig.4d). The overall lack of coarse material suggests these sediments are mostly from the distant and uniform source region suggesting large provenance with variable geological settings which apparently have undergone weak to moderate recycling processes (Ahmad and Chandra, 2013).

Geochemical characterization

For chemical analysis, 46 samples of Kashmir loess-paleosols were analyzed and average composition is presented in Table 1. Major and trace elements were determined by

Sample	**DL1**	**DS1**	**DS3**	**DS4**	**DS6**	**DS7**	**KS1**	**KS2**	**KL1**	**KS7**	**KL2**	**KS10**	**KL3**	**BS1**	**BS4**
SiO_2	51.4	55.17	60.57	56.27	54.05	57.71	58.72	62.97	54.5	62.60	58.21	59.96	63.18	53.9	60.73
Al_2O_3	12.58	13.76	16.47	14.01	14.01	15.43	15.77	16.08	13.95	16.53	15.65	16.13	13.8	13.50	16.30
Fe_2O_3	4.87	5.26	6.78	5.34	5.13	5.81	6.04	6.18	5.34	6.39	5.72	7.02	6.83	5.10	6.756
MnO	0.08	0.08	0.11	0.08	0.08	0.09	0.09	0.10	0.07	0.11	0.091	0.10	0.07	0.08	0.08
MgO	2.59	2.77	2.55	2.73	2.69	2.52	2.62	2.52	2.58	2.36	2.65	2.40	2.62	2.52	2.59
CaO	8.6	6.55	1.31	6.36	6.83	4.06	3.06	1.51	6.33	1.09	3.87	1.97	3.08	7.02	1.43
Na_2O	0.87	0.94	0.92	0.96	0.81	0.78	1.00	1.15	0.81	0.88	0.97	0.92	1.36	0.80	0.91
K_2O	2.68	2.79	3.11	2.78	2.71	2.92	2.87	2.89	2.73	2.89	2.87	2.43	1.86	2.92	2.64
TiO_2	0.6	0.63	0.78	0.64	0.63	0.72	0.71	0.78	0.65	0.79	0.69	0.91	0.99	0.64	0.94
P_2O_5	0.128	0.12	0.10	0.11	0.12	0.10	0.14	0.12	0.12	0.11	0.139	0.11	0.12	0.12	0.09
LOI	14.81	11.41	7.95	10.70	12.25	9.7	9.26	7.10	11.74	7.84	8.33	7.08	5.73	12.5	7.73
Total	99.20	99.51	100.6	100	99.31	99.85	100.3	101.4	98.88	101.6	99.19	99.08	99.65	99.14	100.2

Rb	100.9	112.4	152.0	112.3	106.5	125.8	127.2	140.4	108.4	141	128.1	105.6	68.06	114.7	110.8
Sr	142.3	143.5	112.5	136.6	146.6	155.7	116.8	114.0	146.3	106.6	135.6	133.6	149.8	139.5	108.2
Y	24.40	27.21	32.65	25.87	25.97	33.45	32.56	33.65	28.49	33.73	31.12	34.68	31.61	26.42	37.59
Zr	162.1	180.9	208.1	182.2	178.9	201.2	204.2	223.4	179.6	230.2	207.6	234.4	205	172.1	295.1
Nb	14.30	14.61	18.25	14.48	14.55	16.39	17.17	18.67	15	18.41	16.73	19.41	19.88	14.45	19.36
Ba	374.1	406.1	557	412.1	393.1	471.1	474.1	519.2	391	508.9	478.1	433.2	306.3	395.4	447.8
Ni	41.82	44.56	58.67	44.95	43.19	46.56	53.11	50.97	48.2	55.24	43.47	45.61	35.84	42.40	45.41
Cu	43.24	45.96	52.84	44.19	43.11	45.95	47.39	46.76	47.3	49.50	48.31	45.76	42.52	49.34	45.90
Zn	74.43	78.13	102.3	75.37	75.87	84.61	88.58	85.68	85.1	100.3	86.08	86.56	71.21	89.33	77.70
Ga	12.06	13.17	17.53	12.89	11.89	14.40	14.94	16.27	12.6	15.95	14.18	15.72	13.44	11.92	14.66
Pb	17.05	20.22	23.64	20.35	19.79	20.44	22.33	21.38	19	21.02	20.31	18.99	13.44	21.44	21.69
Th	10.96	13.70	16.41	12.74	12.97	17.36	16.73	18.69	12.5	15.33	16.90	12.73	8.02	11.26	15.94
U	2.98	3.84	6.45	5.06	7.35	8.48	5.49	7.53	5.64	5.78	4.81	6.62	3.82	0.949	4.41
Sc	12.39	12.97	14.99	13.24	13.29	15.39	13.81	14.39	13.44		-	-	-	13.93	16.66
V	189.3	89.33	100.8	99.56	93.26	110	107.3	112.6	99.91	-	-	-	-	103.7	135.5
Co	15.04	16.09	18.25	16.5	15.93	17.34	17.56	19.4	17.27	-	-	-	-	18.21	21.45
Hf	2.09	2.32	2.72	2.5	2	3	2.64	3.675	3	-	-	-	-	1.87	3
La	34.13	37.12	41.51	37.87	37.18	41.59	40.18	45.36	38.13	-	-	-	-	42.63	49.4
Ce	66.28	72.87	82.1	72.72	72.36	79.68	78.04	87.01	69.42	-	-	-	-	79.55	93.28
Pr	7.26	8.10	9.19	8.21	8.01	9.25	9.015	10.21	8.26	-	-	-	-	8.91	10.28
Nd	26.71	30.07	33.72	30.05	28.92	33.74	34.44	39.69	32.5	-	-	-	-	31.91	39.43
Sm	5.5	6.7	6.89	6.75	6.99	7.21	6.79	7.26	6.72	-	-	-	-	6.51	7.77
Eu	1.33	1.54	1.61	1.57	1.42	1.8	1.58	1.65	1.55	-	-	-	-	1.55	1.82
Gd	4.83	5.05	5.72	5.2	5.07	6.25	5.62	6.16	5.36	-	-	-	-	5.57	6.61
Tb	0.71	0.73	0.84	0.74	0.73	0.93	0.80	0.87	0.76	-	-	-	-	0.82	0.94
Dy	3.85	4.02	4.64	4.05	4.09	5.02	4.59	5.12	4.34	-	-	-	-	4.22	4.99
Ho	0.96	0.99	1.16	1	0.99	1.25	1.10	1.19	1.07	-	-	-	-	1.05	1.3
Er	2.2	2.21	2.60	2.31	2.27	2.83	2.48	2.67	2.3	-	-	-	-	2.45	2.94
Tm	0.37	0.37	0.43	0.38	0.37	0.47	0.41	0.45	0.4	-	-	-	-	0.4	0.47
Yb	2	2	2.30	2.02	2.02	2.44	2.18	2.24	2.05	-	-	-	-	2.14	2.30
Lu	0.26	0.25	0.3	0.25	0.26	0.32	0.29	0.31	0.26	-	-	-	-	0.29	0.33
CIA	68.58	69.02	71.97	69.11	71.44	72.93	71.07	69.89	71.28	73.16	71.3	74	68.02	69.87	73.55
CIW	81.46	81.49	84.43	81.36	84.01	85.73	82.71	80.88	83.96	84.95	83.06	84.15	75.51	83.57	84.46

Table 1. Average geochemical composition of loess-paleosol sediments of Kashmir valley, India. using X-Rays Fluorescence (XRF) spectrometer and REE with some trace elements were determined by ICP-MS at Wadia Institute of Himalayan Geology (WIHG), Dehradun, India. The accuracy of the analytical method was established using two internationally recognized standard reference materials: MAG-I and MAG (R.V). Loss on ignition (LOI) was calculated as a percentage of dry weight after the samples were ignited at 950°C for 24 hour.

To evaluate the nature of the Kashmir Loess-Paleosol sediments and chemical behavior of major oxides during pedogenic process, the concentration of major oxides is also plotted in Upper Continental Crust (UCC) normalized spider diagrams (Fig.5). SiO_2 and Al_2O_3 wt% show constant proportions and generally follow the similar trend to that of UCC, PAAS and NASC. This suggests warm semi-arid climatic conditions because these elements remain stable under semi-arid climate (Guo, 2010). However, the UCC normalized Fe_2O_3, MnO and MgO wt% show slightly higher concentration than the UCC but follow similar pattern to that of PAAS. This suggests that the ferromagnesian minerals are least affected by the pedogenic modification.

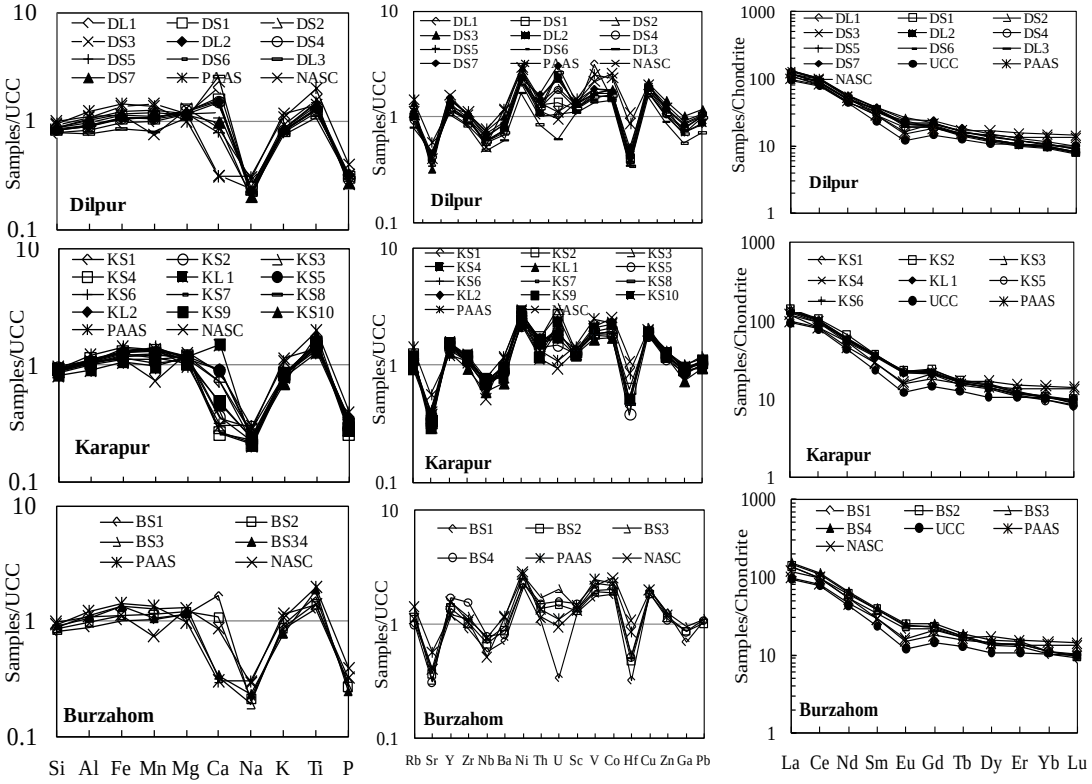

Fig.5. *UCC normalized spider diagrams for major oxides and trace elements composition of Kashmir Loess-Paleosol sediments at Dilpur, Karapur and Burzahom Village sections, (PAAS and UCC values after Taylor and McLennan, 1985; NASC values after Gromet et al. 1984). Also shown are the **c**hondrite normalized REE patterns for these sediments. All the major oxides are as oxides wt%.*

All the three sections show almost similar concentration of K_2O wt%, which is generally lower than the UCC, PAAS and NASC. The negative anomalies of Na_2O followed by K_2O wt% (Fig.5) indicate relatively more alteration of plagioclase feldspar than the K-feldspar. However, CaO wt% shows wide range of variation in its concentrations with respect to UCC. It is well known that the CaO contents of loess varies greatly and shows both positive and negative anomalies on UCC normalized spider diagrams (Gallet et al. 1998). The wide range of variations in CaO wt% may be argued for high LOI, which ranges from 5.71 to 14.8 wt% (Honda et al. 2004). The lower values of CaO wt% relative to PAAS indicate an intense mobilization during post depositional processes, whereas high values indicate that these sediments are relatively less mature than the PAAS (Mahjoor et al. 2009). TiO_2 wt% contents are significantly higher than the UCC. However, it is slightly lower than the PAAS. The enrichment of TiO_2 wt% is generally ascribed to the presence of Ti-bearing phyllosilicates (biotite and chlorite). These minerals generally reside in fine clay sediments. It also suggests significant contribution from the mafic source rocks. The positive correlation between ΣREE and Al_2O_3 contents (r = 0.81) also indicates that the REE are mostly concentrated in the fine clay fraction. This suggests significant proportion of clay minerals in the Kashmir Loess-Paleosol sediments.

To evaluate the nature and chemical behavior of various trace elements during pedogenic process, the average concentration of trace elements is also plotted in Upper Continental Crust (UCC) normalized spider diagrams (Fig.5). The Sr shows negative correlations (r = −0.68) with SiO_2 (wt%) which indicates that the sediments are depleted in carbonate minerals. SiO_2 show positive correlation with Ba (r = 0.66) and Rb (r = 0.50) suggesting their robustness during pedogenesis. The Rb and Sr show different geochemical behavior during pedogenesis. The relatively higher concentration of Rb indicates that mica and K-feldspar are not strongly affected by the pedogenesis. The weathering of plagioclase decreases the concentration of Sr because Sr is more mobile than the Ba.

Rb/Sr ratio shows higher concentration in paleosols than the altered loessic layers. Ba/Sr ratio also follows the similar trend (Fig.6). This ratio has been considered as related to the leaching intensity (Gallet et al. 1996). High peaks of Rb/Sr and Ba/Sr in paleosols are the result of land surface stability during the warm and wet periods which accelerate pedogenesis (Gallet et al. 1996). The diagram also used to correlate the lithostratigraphy of Kashmir Loess-Paleosol sediments. The pedocomplex between DL1–DL2 (0m−8.5m) at Dilpur is stratigraphically equivalent to the KS1−KL1 (0m−8.7m) at Karapur. The whole Burzahom section is stratigraphically equivalent to this pedocomplex. The pedocomplex between DL2−DL3 represents another warm-wet period. It is stratigraphically equivalent to KL1−KL2. The other small peaks represent the minor fluctuations in precipitation conditions. The increase in concentration of CaO (wt%) upward suggests the increasing aridity during the close of Pleistocene Period. Similar patterns are also observed for Al_2O_3/SiO_2, $(Al_2O_3 + Fe_2O_3)/(Na_2O+K_2O+MgO+P_2O_5)$, $Al_2O_3/(CaO+Na_2O+K_2O)$, Fe_2O_3/CaO and Fe_2O_3/Al_2O_3 (not included here). Further, the ratios of immobile elements such as La/Co, Zr/Y and Zr/Hf, show no correlation with Al_2O_3 (−0.49, 0.0029, 0.075 respectively) and CIA values (−0.57, −0.0366 and 0.051 respectively) which suggest that these elements are resistant to chemical weathering. The whole Burzahom section is stratigraphically equivalent to this pedocomplex.

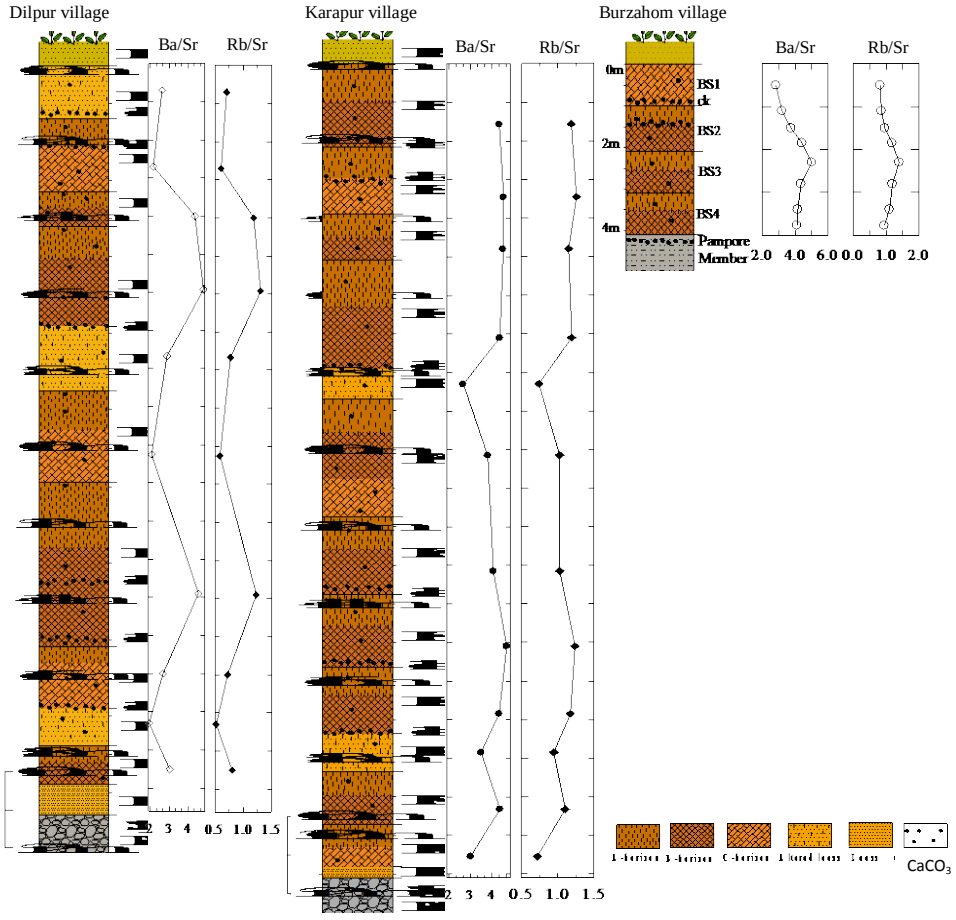

Fig.6. *Showing variations of Ba/Sr (ppm) and Rb/Sr (ppm) with stratigraphic depth in Kashmir Loess-Paleosol sediments at Dilpur, Karapur and Burzahom Village sections.*

The pedocomplex between DL2−DL3 represents another warm-wet period. It is stratigraphically equivalent to KL1−KL2. The other small peaks represent the minor fluctuations in precipitation conditions. The increase in concentration of CaO (wt%) upward suggests the increasing aridity during the close of Pleistocene Period. Similar patterns are also observed for Al_2O_3 / SiO_2, (Al_2O_3 + Fe_2O_3) / (Na_2O + K_2O + MgO + P_2O_5), Al_2O_3 / (CaO+Na_2O+K_2O), Fe_2O_3/CaO and Fe_2O_3/Al_2O_3 (not included here). Further, the ratios of immobile elements such as La/Co, Zr/Y and Zr/Hf, show no correlation with Al_2O_3 (–0.49, 0.0029, 0.075 respectively) and CIA values (–0.57, –0.0366 and 0.051 respectively) which suggest that these elements are resistant to chemical weathering.

The Chondrite normalized REE patterns are plotted in Fig.5. These are characterized by moderate enrichment of LREEs, relatively flat HREE pattern (Gd_{CN}/Yb_{CN} = 1.93 to 2.30), lack of prominent negative Eu anomaly (Eu/Eu* = 0.73 to 1.01, average = 0.81) and variable amount of ∑REE. The Eu and Ce anomalies in the samples are determined according to: $Eu/Eu^* = (Eu_{CN}) / \{(Sm_{CN}) \times (Gd_{CN})\}^{0.5}$ and $Ce/Ce^* = (Ce_{CN}) / \{(La_{CN})^{0.666} \times (Nd_{CN})^{0.333}$. Eu anomaly ranges between 0.73 and 1.01 (average = 0.81). In contrast, nearly half of the samples show positive Ce anomaly and it ranges from 0.92 - 1.04 (average = 0.99. The La_{CN}/Yb_{CN} ratio of the studied samples do not correlates with the weathering indices (CIW vs La_{CN} / Yb_{CN}; r = 0.090 and PIA vs La_{CN} / $Yb_{CN;}$ r = 0.14). Further, the absence of correlation between Eu/Eu* vs Al_2O_3 (−0.29) and Eu/Eu* vs CIA (−0.38) indicates that chemical weathering did not fractionate LREE from HREE. This lack of evidence of intense weathering at the source depicted by the LREE/HREE (La_{CN}/Yb_{CN}) ratios suggests that the REEs are not subjected to weathering (Cai et al. 2008). Hence, REE pattern of the studied samples is mainly inherited from the source provenance.

Weathering Intensity

To know the extent of pedogenesis, Chemical Index of Alteration (CIA), proposed by Nesbitt and Young (1982) have been calculated. This index used to determine the proportion of primary minerals and the transformation of feldspars to secondary clay minerals relative to the fresh parent material. Hence CIA value provides an accurate measurement of degree of weathering and it can be obtained by using molecular proportions: CIA = (Al_2O_3 /Al_2O_3 + CaO* +Na_2O+K_2O) ×100. CaO* represents the CaO in silicates bearing minerals. The CIA value of Kashmir Loess-Paleosol sediments ranges from 67.13 to 75.27 (Table-I). This narrow and restricted range of CIA value shows moderate degree of weathering, suggesting dry and cold climate during deposition (Nesbitt and Young, 1982). According to Taylor and McLennan (1985), the moderate weathering suggests that the effect of weathering had not advanced to the stage where alkali and alkaline earth elements are substantially removed from the soil. Chemical index of weathering (CIW) proposed by Harnois (1988) also used to determine the degree of weathering and it can be obtained by using molecular proportions. CIW = (Al_2O_3 /Al_2O_3 + CaO* +Na_2O) × 100. CIW values of these samples range from 79.93−88.63, suggesting moderate degree of weathering. The consistency of CIA with CIW values indicate that the degree of pedogenesis operated on the Kashmir Loess-Paleosol is moderate. Ternary A−CN−K diagram {Al_2O_3− (CaO* + Na_2O) − K_2O) also used to deduce the weathering trend (Nesbitt and Young, 1982). In this diagram (A = Al_2O_3; CN = CaO* + Na_2O; K = K_2O), the loess-paleosol sediments plot above plagioclase-potash feldspar line (Fig.7), and clustered close to the PAAS and NASC and fall intermediate between A–CN and A–K lines, which show weak to intermediate removal of Ca and Na (Buggle et al. 2008). The plots do not exhibit any inclination towards the K apex indicating that the loess-paleosol sediments were not subjected to potash metasomatism (Moosavirad et al. 2010).

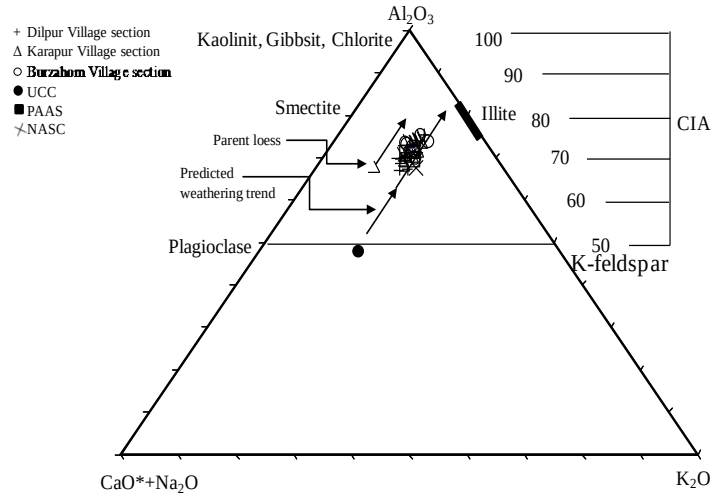

Fig. 7. *A–CN–K ternary diagram for the Kashmir Loess-Paleosol sediments (after Nesbitt and Young, 1984), also plotted are the average UCC, PAAS (Taylor and McLennan, 1985) and NASC (after Gromet et al., 1984) values as well as some rock forming minerals important in silicate rock weathering; shown at the side is the CIA scale. The Kashmir Loess-Paleosol sediments fall closer to moderately weathered minerals.*

Therefore, use of CIA index in weathering studies assumes that this index is a measurement of the amount of the chemical weathering. However, other factors that may affect the CIA value and need to be taken into account include sediment provenance and post-depositional processes that lead to K^+ addition (e.g. diagenetic illitization and metasomatism). Sedimentary sorting can significantly influence the chemical composition of terrigenous sediments due to grain size and mineral sorting (Bauluz et al. 2000). For instance, aluminum is concentrated in the clays, hence the larger the transport (i.e. distal regions), the finer the sediments and the higher the Al concentration (Soreghan and Soreghan, 2007). There is also a tendency of larger grain sizes to concentrate feldspars, which leads to lower CIA values (Zimmerman and Bahlburg, 2003). Therefore, the use of the CIA as a weathering index, however, can be limited by the inheritance of clays from sedimentary rocks in the source area. However, in this study it reveals that these sediments are enriched in rock forming minerals with significant proportion of clays, indicating that CIA value to some extent is affected by these clays. In addition, the A-CN-K diagram (Fig.7) also indicates that these loess-paleosol sediments are not subjected to potash metasomatism. Therefore, weathering intensity inferred by these proxies indicating moderate degree of weathering, probably suggest combined result of weathering and grain size effect due to transportation processes. Hence, on the bases of these geochemical observations it is proposed that the Kashmir Loess-Paleosol sediments experienced weak to moderate degree of weathering.

Conclusion

Integrated micromorphological and geochemical study of the Quaternary Loess-Paleosols sediments of the Kashmir Valley revealed that all these sediments are characterized by similar pedofeatures irrespective of horizon types suggesting syndepositional origin of loess deposits and weak to moderate weathering. It further suggests that loess deposition and pedogenesis is likely competing processes and neither stop completely during either phase of the loess/soil formation. Chemically, these sediments also show similar compositions and alteration history. Only mobile elements Ca, Na, P and Sr are depleted in these sediments. Chondrite normalized REE patterns are characterized by moderate enrichment of LREEs, relatively flat HREE pattern (Gd_{CN}/Yb_{CN} = 1.93 to 2.30), lack of prominent negative Eu anomaly (Eu/Eu* = 0.73 to 1.01, average = 0.81) and variable amount of total REE (∑REE = 156.1 to 226.43). The weathering indices (CIA, CIW and A-CN-K diagram) and others elemental ratios suggest that these sediments experienced weak to moderate degree of chemical weathering and not subjected to potash metasomatism during diagenesis. Ratios of various major and trace elements suggest that Middle to Late Pleistocene period is defined by several episodes of pedogenic activity representing warm arid to semi arid climatic conditions in the valley. This is further supported by the clay mineralogical study of these sediments which indicates that these sediments are enriched with smectite with lower concentration of mixed-layered chlorite + kaolinite (c+k) and traces of illite clay minerals (not included here).

Acknowledgements

The authors are thankful to Head of Department, Department of Earth Sciences, University of Kashmir, Srinagar, J&K, India and Director, Wadia Institute of Himalayan Geology (WIHG),

Dehradun, India for providing laboratory and analytical facilities for generating micromorphological and geochemical data.

References:

Ishtiaq Ahmad 2012. Geochemical study of loess-paleosol Quaternary sediments of Karewa Basin with reference to paleoclimate of Kashmir valley, J&K, India. Ph.D. Thesis, Department of Earth Sciences, University of Kashmir, India.

Ishtiaq Ahmad and Rakesh Chandra. Geochemistry of loess-paleosol sediments of Kashmir Valley, India: Provenance and weathering. J. Asian Earth Science 66, 73-89, 2013.

B. Bauluz, M. J. Mayayo, C. Fernandez-Nieto, and J. M. G Lopez. Geochemistry of Precambrian and Paleozoic siliciclastic rocks from the Iberian Range (NE Spain): implications for source-area weathering, sorting, provenance and tectonic setting. Chemical Geology 168, 135–150, 2000.

M. I. Bhat, and S. M. Zainuddin. Origin and evolution of Panjal volcanics. Himalayan Geology 9, 421-461, 1979.

A. Bronger, R. K. Pant, A. K. Singhvi. Pleistocene climatic changes and landscape evolution in the Kashmir Basin, India: Paleopedologic and Chronostratigraphic studies. Quaternary Research 27, 167-181, 1987.

B. Buggle, B. Glaser, L. Zoller, U. Hambach, S. Markovic, I. Glaser, and N. Gerasimenko. Geochemical characterization and origin of Southeastern and Eastern European loesses (Serbia, Romania, Ukraine). Quaternary Science Reviews 27, 1058–1075, 2008.

I. A. Farooqi, and R. N. Desai. Stratigraphy of Karewas, Kashmir, India. Jour. of the Geol. Soc. of India, 1974.

S. Gallet, B. Jahn, and M. Torii. Geochemical characterization of the Luochuan loess-paleosol sequence, China, and paleoclimatic implications. Chemical Geology 133, 67-88, 1996.

S. Gallet, B. Jahn, B. Van Vliet-Lanoe, A. Dia, E. A. Rossello. Loess geochemistry and its implications for particle origin and composition of the upper continental crust. Earth and Planetary Science Letters 156, 157–172.1998.

Z. T. Guo. Loess geochemistry and Cenozoic paleoenvironments. Geoche. News, 143, 1-10, 2010.

R. Gardner. Late Quaternary loess and paleosols, Kashmir Valley, India. Zeitschrift fur Geomorphologie Supplement 6, 225-245, 1989.

L. P. Gromet, R. F. Dymek, L. A. Haskin, R. L. Korotev. The North American Shale Composite: its compilation, major and trace element characteristics. Geochimica et Cosmochimica Acta 48, 2469–2482, 1984.

S. K. Gupta, P. Sharma, N. Juyal, and D.P. Agrawal. Loess-paleosol sequence in Kashmir: correlation of mineral magnetic stratigraphy with the marine paleoclimatic record. Journal of Quaternary Science 6, 3-12, 1991.

M. Honda, S. Yabuki, and H. Shimizu. Geochemical and isotopic studies of aeolian sediments in China. Sedimentology 51, 211–230, 2004.

L. Harnois. The CIW index: A new chemical index of weathering. Sedimentary Geology 55, 319–322, 1988.

R. A. Kemp, and M. A. Zarate. Pliocene pedosedimentary cycles in the Southern Pampas, Argentina. Sedimentology 47, 3-14, 2000.

R. A. Kemp, P.S. Toms, J. M. Sayago, E. Derbyshire, M. King, and L. Wagoner. Micromorphology and OSL dating of the basal part of the loess–paleosol sequence at La Mesada in Tucumán province, Northwest Argentina. Quaternary International 106/107, 111–117, 2003.

J. J. Li, J. J. Zhu, J. C. Kang, F. H. Chen, X. M. Fang, D. F. Mu, J. X. Cao, L. S. Tang, Y. T. Zhang, and B. T. Pan. Comparison of Lanzhou loess section of last glacial epoch with Antarctic Vostok ice core. Science in China Bulletin 35, 476-487, 1992.

A. S. Mahjoor, M. Karimi, and A. Rastegarlari. Mineralogical and geochemical characteristics of clay deposits (Central Iran) and their applications. Journal Applied Science 9, 601-614, 2009.

S. M. Moosavirad, M. R. Janardhana, M. S. Sethumadhav, M. R. Moghadam, and M. Shankara. Geochemistry of lower Jurassic shales of the Shemshak Formation, Kerman Province, Central Iran: Provenance, source weathering and tectonic setting. Chemie der Erde-Geochemistry 2011.

H. W. Nesbitt, and G. M. Young. Early Proterozoic climates and plate motion inferred from major element chemistry of lutites. Nature 299, 715-717, 1982.

A. K. Singhvi, A. Bronger, R. K. Pant, W. Sauer. Thermoluminescence dating and its implications for the chronostratigraphy of loess-paleosol sequences in the Kashmir Valley, India. Chemical Geology 65, 45-56, 1987.
M. J. Soreghan, and G. S Soreghan. Whole-rock geochemistry of upper Paleozoic loessite, western Pangaea: implications for paleoatmospheric circulation. Earth and Planetary Science Letters 255, 117–132, 2007.
S. R. Taylor, and S. M. McLennan. The Continental Crust: Its composition and evolution. Blackwell, Oxford, 312pp, 1985.
V. C. Thakur, and B. S. Rawat. Geological map of the Western Himalaya. Published under the authority of the Surveyor General of India. Printing Group of Survey of India, 101 (HLO), 1992.
E. Yakimenko, S. Inozemtsev, S. Naugolnykh. Upper Permian paleosols (Salarevskian Formation) in the central part of the Russian Platform: Paleoecology and paleoenvironment. Revista Mexicana de Ciencias Geologicas 21, 110-119, 2004.
M. Zarate, R. A. Kemp, M. Espinosa, and L. Ferrero. Pedosedimentary and paleoenvironmental significance of a Holocene alluvial sequence in the southern Pampas, Argentina. The Holocene 10, 481-488, 2000.
G. Zhengtang, N. Fedoroff, L. Dongsheng. Micromorphology of the loess-paleosol sequence of the last 130 ka in China and paleoclimatic events. Science in China D 29, 468-477, 1996.
U. Zimmerman, and H. Bahlburg. Provenance analysis and tectonic setting of the Ordovician clastic deposits in the southern Puna Basin, NW Argentina. Sedimentology 50, 1079-1104, 2003.